Cell Biology International ISSN 1065-6995
doi: 10.1002/cbin.10343

RESEARCH ARTICLE

Epigallocatechin-3-gallate suppresses the lipid deposition through the apoptosis during differentiation in bovine bone marrow mesenchymal stem cells

Jin Young Jeong[1], Sekar Suresh[1], Mi Jang[1], Mi Na Park[1], Kuppannan Gobianand[1], Seungkwon You[2], Sung-Heom Yeon[1] and Hyun-Jeong Lee[1]*

1 Division of Animal Genomics and Bioinformatics, National Institute of Animal Science, Rural Development Administration, #564 Omockchun-dong, Suwon 441-706, Republic of Korea
2 The Laboratory of Cell Growth and Function Regulation, Division of Bioscience and Technology, College of Life and Environmental Sciences, Korea University, Seoul 136-701, Republic of Korea

Abstract

Epigallocatechin gallate (EGCG), a major component of tea, has known effects on obesity, fatty liver, and obesity-related cancer. We explored the effects of EGCG on the differentiation of bovine mesenchymal stem cells (BMSCs, which are multipotent) in a dose- and time-dependent manner. Differentiating BMSCs were exposed to various concentrations of EGCG (0, 10, 50, 100, and 200 μM) for 2, 4, and 6 days. BMSCs were cultured in Dulbecco's modified Eagle's medium (DMEM)/high-glucose medium with adipogenic inducers for 6 days, and the expression levels of various genes involved in adipogenesis were measured using real-time polymerase chain reaction (PCR) and Western blotting. We assessed apoptosis by flow cytometry and terminal deoxynucleotidyl transferase dUTP nick-end labeling (TUNEL) staining of control and EGCG-exposed cells. We found that EGCG significantly suppressed fat deposition and cell viability ($P < 0.05$). The mRNA and protein levels of various adipogenic factors were measured. Expression of the genes encoding peroxisome proliferator-activated receptor gamma (PPARG), CCAAT/enhancer-binding protein alpha (CEBPA), fatty acid-binding protein 4 (FABP4), and stearoyl-CoA desaturase (SCD) were diminished by EGCG during adipogenic differentiation ($P < 0.05$). We also found that EGCG lowered the expression levels of the adipogenic proteins encoded by these genes ($P < 0.05$). EGCG induced apoptosis during adipogenic differentiation ($P < 0.05$). Thus, exposure to EGCG potentially inhibits adipogenesis by triggering apoptosis; the data suggest that EGCG inhibits adipogenic differentiation in BMSCs.

Keywords: adipogenic factor; apoptosis; BMSC; differentiation; EGCG

Introduction

Global trends toward excessive fat deposition and obesity are consistently linked to increased incidences of diabetes, fatty liver disease, cancer, and heart disease, and epigallocatechin-3-gallate (EGCG), a widely consumed polyphenolic component abundant in tea, is recognized to have therapeutic potential in preventing HIV, cancers, arthritis, neurodegeneration, diabetes, and obesity (Yang et al., 2012; Moseley et al., 2013; Renno et al., 2013; Toolsee et al., 2013; Valenti et al., 2013; Byun et al., 2014). EGCG use affects body weight, and energy and lipoprotein levels (Basu et al., 2010; Mielgo-Ayuso et al., 2013). EGCG regulates thermogenesis, fatty oxidation in obese men (Boschmann and Thielecke, 2007), and the activities of various lipogenic enzymes (Huang et al., 2009). EGCG also controls the expression of resistin and inhibits adipogenic differentiation by 3T3-L1 cells (Liu et al., 2006). The beef industry faces the challenge that it must reduce the fat content in meat carcasses in order to decrease the amount of inedible fat without affecting beef quality. Therefore, fat metabolic mechanisms and nutrition modifying technologies needs to manipulating fat deposition in cattle.

Mesenchymal stem cells (MSCs) are known multipotent progenitor cells, and human MSCs can be readily isolated

*Corresponding author: email: hyunj68@korea.kr
Jin Young Jeong and Sekar Suresh have contributed equally to this work.

Cell Biol Int 39 (2015) 52–64

from bone marrow (Menssen et al., 2011), which differentiate under appropriate conditions into adipocytes, osteoblasts, or chondrocytes (Doherty et al., 1998; Farrington-Rock et al., 2004; Collett and Canfield, 2005). MSCs have been isolated from the bone marrow of many mammals, including laboratory rodents (Friedenstein et al., 1974, 1976; Simmons et al., 1991) and humans (Pittenger et al., 1999). However, bovine MSCs (BMSCs) are not often used as an experimental model, although they may be useful in the development of new therapies and disease models.

Adipogenesis, a commonly studied model of differentiation, is associated with changes in cellular, morphological, and physiological characteristics, and adipocytes are derived from multipotent MSCs that have the capacity to develop into several cell types (e.g., adipocytes, myocytes, chondrocytes, and osteocytes). These stem cells reside in the vascular stroma of adipose tissue as well as in bone marrow. EGCG inhibits adipogenesis during differentiation of 3T3-L1 cells (Ku et al., 2009; Chan et al., 2011; Lee et al., 2013), and adipose tissue may represent a valuable source of stem cells (Zuk et al., 2002). Stem cell populations having a wide biological potential have been isolated from human adipose tissue (Zuk et al., 2002; Aust et al., 2004; Schreml et al., 2009). MSCs from bone marrow can differentiate into lineages characteristic of other tissues (Boeloni et al., 2009; Geng et al., 2009). CEBPA and PPARG are transcription factors important in adipogenesis, and FABP4 and SCD serve as positive regulators as PPARG target genes to induce adipocyte differentiation (Proctor et al., 2006; Shin et al., 2009). Because any effect of EGCG on adipogenesis of BMSCs remains clear, our objective has been to determine if EGCG had an anti-adipogenic potential and to examine the expression levels of candidate adipogenic genes and proteins during adipogenic differentiation of BMSCs. We found that an increase in apoptosis may be a key feature of the anti-adipogenic action exerted by EGCG during differentiation.

Materials and methods

Isolation of BMSCs, adipogenic induction, and EGCG exposure

The BMSC line was established from normal bone marrow mesenchymal cells of a 10-week-old fetus of Korean cattle (Hanwoo). The bone marrow was extracted from the proximal and distal ends of the femur into a saline solution with penicillin (1000 U/mL), streptomycin (500 μg/mL), and amphotericin B (2 μg/mL). The tissue was minced and disaggregated in 0.25% (w/v) trypsin–ethylenediaminetetraacetic acid (EDTA; Gibco-BRL, Grand Island, NY) at 37 °C for 2 h. The cells were grown in minimum essential medium (MEM; Gibco-BRL) supplemented with 5% (v/v) fetal bovine serum (FBS; Gibco-BRL) with antibiotics and subcultured when the cells attained confluence. After the fifth passage, cells were grown in high-glucose Dulbecco's modified Eagle's medium (DMEM) supplemented with 10% (v/v) FBS and 2 mM l-glutamine. Cells were infected with retroviruses expressing pBABESV40LT-Puro and pBABE-hTERT-Neo prepared from the PT67 amphotropic packaging cell line (Clontech, Mountain View, CA), after which selection with puromycin (1 μg/mL) was performed for 7 days and selection with G418 (400 μg/mL) for 14 days. Cell senescence was assayed with the aid of a senescence-associated β-galactosidase (SA-β-gal) assay kit. Relative cell growth was determined by staining with 0.01% (w/v) crystal violet. To explore the DNA damage response (DDR) of primary BMSCs, cells were grown in the absence/presence (1 and 10 μM) of doxorubicin for 18 h. Some cells were transferred to DMEM containing 30% (v/v) FBS and 10% (v/v) dimethyl sulfoxide (DMSO). The remaining cells were immediately frozen in liquid nitrogen. Cells were seeded into 12-well plates and grown until 80% confluence was attained. Differentiation was induced using an adipogenic cocktail containing 10 μg/mL insulin, 5 μM dexamethasone, and 0.5 mM 3-isobutyl-1-methylxanthine (IBMX). The cells were treated with various concentrations (10, 50, 100, and 200 μM) of EGCG during differentiation. The medium was changed every 2 days for 6 days, and cells were harvested at different times (2, 4, and 6 days) after induction of differentiation.

Measurement of cell viabilty

3-(4,5-dimethylthiazol-2-yl)-2,5-diphenyltetrazolium bromide (MTT) assay was used to determine the effect of EGCG on the growth and viability of differentiating BMSCs. Cell viability was measured using an MTT assay kit (Sigma-Aldrich, St. Louis, MO). Briefly, cells (1×10^5/well) were seeded into 12-well plates and cultivated in 100 μL amounts of medium for 24 h. After attaining 80% confluence, cells were treated with EGCG (10, 50, 100, and 200 μM). At 2, 4, and 6 days post-treatment, they were assayed with MTT. Finally, the absorbance of each well at 570 nm was measured using a Countess® automated cell counter (Invitrogen, Carlsbad, CA).

Oil red O staining and Quantification

BMSCs differentiating in the presence of EGCG (or not) were stained with Oil Red O. Briefly, cells were rinsed twice with phosphate-buffered saline (PBS, pH 7.4) and fixed in 10% (v/v) formalin in PBS for 20 min, washed with 60% (v/v) isopropyl alcohol, and stained in 2% (w/v) Oil Red O (Sigma-Aldrich) for 30 min at room temperature. Cells were washed in isopropyl alcohol followed by repeated washes in distilled water. Staining was also quantified by extraction of Oil Red O into 100% isopropyl alcohol. Absorbance was measured at

510 nm. The number of total cells per field was determined by fluorescence microscopy followed by determination of the number of cells containing Oil Red O-stained inclusions. A cell containing a visibly stained vacuole was considered to be positively stained. Additionally, for each view, the percentage area of positive staining was determined using ImageJ software (NIH, Bethesda, MD). The area stained was determined by quantifying the actual area stained rather than the area covered by cells containing stained vacuoles.

Measuring apoptotic cell numbers by flow cytometry

BMSCs were seeded into 12-well plates (1.5×10^5 cells/well). Cells were maintained in medium with 10% (v/v) FBS and various concentrations of EGCG. The apoptotic effect of EGCG on differentiating BMSCs was evaluated using an Annexin V staining kit (Sigma-Aldrich). Cells were collected via trypsinization and stained. Flow cytometric analysis involved a FACSCalibur^{TM} platform (BD Biosciences, Franklin Lakes, NJ).

TUNEL assays

To confirm that cell death followed an apoptosis-like mechanism upon exposure to EGCG, we used an In Situ Cell Death Detection Kit (Roche Applied Science, Indianapolis, IN). Briefly, after incubation with the terminal deoxynucleotidyl transferase dUTP nick-end labeling (TUNEL) mixture, cells were rinsed three times with PBS, embedded in an antifade matrix, and examined under a fluorescence microscope using excitation and emission wavelengths of 570 nm and 620 nm, respectively.

Immunocytochemistry

BMSCs were cultured on coverslip as 1×10^5 cells for immunocytochemistry according to the method described by Glynn and McAllister (2006). After the EGCG exposure, the cells was fixed with 4% paraformaldehyde in PBS for 30 min at RT, permeabilized with 0.2% Triton-X in PBS for 10 min at RT. The non-specific site was blocked with blocking buffer (2% bovine serum albumin) for 30 min at RT. The cells were incubated with rabbit polyclonal PPARG and SCD (1:200) antibodies at 4 °C. After wash with PBS, the cells were incubated with secondary antibodies (goat anti rabbit IGg conjugated with FITC and TR). The cells were mounted with anti-fade solution containing the DAPI (Invitrogen) and analyzed under fluorescent microscopy with appropriate filters.

RNA extraction and real-time PCR analysis

BMSCs were harvested after 0, 2, 4, and 6 days of adipogenic differentiation. Total RNA was extracted using the TRIzol reagent (Molecular Research Center, Cincinnati, OH). Total RNA levels were quantified by absorbance at 260 nm, and RNA integrity was checked by 1% (w/v) agarose gel electrophoresis followed by ethidium bromide staining of the 28 S and 18 S bands.

Total RNA (1 μg amounts) was reverse-transcribed into cDNA using an iScript cDNA Synthesis kit (Bio-Rad, Hercules, CA) according to the manufacturer's instructions. Real-time PCR was performed using QuantiTect SYBR Green RT-PCR Master Mix (Qiagen, Valencia, CA) and a 7500 Fast Sequence Detection System (Applied Biosystems, Foster City, CA). Briefly, PCR was done in a final reaction volume of 25 μL containing 200 ng cDNA, 12.5 μL SYBR Green RT-PCR Master Mix, and 1.25 μL of each of two primer solutions (10 μM). The thermal cycling parameters were as follows: 50 °C for 2 min and 95 °C for 15 min followed by 40 cycles at 94 °C for 15 s, 62 °C for 30 s, and 72 °C for 30 s. All primers were designed by reference to sequences published by the National Center for Biotechnology Information (Table 1). The $2^{-\Delta\Delta Ct}$ method was used to determine relative fold changes in mRNA levels (Livak and Schmittgen, 2001). All data were normalized to the

Table 1 Primer sequences used in real-time PCR.

Gene name, Symbol	GenBank ID	5′ → 3′	Sequence	Amplicon size, bp
CCAAT/enhancer binding protein (C/EBP), alpha, CEBPA	NM176784	Forward	tggacaagaacagcaacgag	130
		Reverse	ttgtcactggtcagctccag	
Fatty acid binding protein 4, FABP4	NM174314	Forward	ggatggaaaatcaaccacca	84
		Reverse	gtggcagtgacaccattcat	
Peroxisome proliferator-activated receptor gamma, PPARG	BC116098	Forward	aggatggggtcctcatatcc	121
		Reverse	gcgttgaacttcacagcaaa	
Stearoyl-CoA desaturase, SCD	AF188710	Forward	cgcccttatgacaagaccat	80
		Reverse	tagttgtggaagccctcacc	
Glyceraldehyde-3-phosphate dehydrogenase, GAPDH*	BC102589	Forward	acccagaagactgtggatgg	125
		Reverse	ttgagctcagggatgacctt	

*Housekeeping gene.

Cell Biol Int **39** (2015) 52–64 © 2014 The Authors. Published by John Wiley & Sons Ltd on behalf of the International Federation for Cell Biology.

expression level of the housekeeping gene glyceraldehyde 3-phosphate dehydrogenase (GAPDH).

Protein extraction and Western blotting

BMSCs were homogenized using a Polytron homogenizer for 10 s in cold Pro-PREP protein extraction solution (Intron, Seongnam, Korea) containing 1 mM phenylmethylsulfonyl fluoride (PMSF), 1 mM EDTA, 1 μM pepstatin A, 1 μM leupeptin, and 0.1 μM aprotinin. Lysates were left at –20 °C for 30 min. After centrifugation at 10,000 × *g* for 10 min at 4 °C, the protein concentration of each supernatant was determined by the Bradford method. Total protein samples were prepared for Western blotting by boiling in 5 × sample buffer [50 mM Tris, 2% (w/v) SDS, 5% (v/v) glycerol, and 10% (v/v) 2-mercapto-ethanol; pH 6.8]. Proteins (50 μg) were separated by molecular mass on 12% (w/v) sodium dodecyl sulfate–polyacrylamide gel electrophoresis (SDS-PAGE) separating gels, with 5% (w/v) polyacrylamide stacking gels, and the expression levels of the following proteins were determined: peroxisome proliferator-activated receptor gamma (PPARG; 58 kDa), fatty acid-binding protein 4 (FABP4; 15 kDa), CCAAT/enhancer-binding protein alpha (CEBPA; 45 kDa), and stearoyl-CoA desaturase (SCD; 40 kDa).

Separated proteins were transferred onto polyvinylidene fluoride (PVDF) membranes (Bio-Rad). The membranes were blocked with 5% (w/v) skim milk in Tris-buffered saline containing 0.1% (v/v) Tween 20 and next incubated with commercial primary antibodies (1:1,000 dilution of antibodies against PPARG, FABP4, and SCD; 1:2,000 dilution of an antibody against CEBPA). In detail, the antibodies were rabbit polyclonal antihuman PPARG (Abcam, Cambridge, UK), rabbit polyoclonal anti-human FABP4 (Abcam), goat polyclonal antihuman SCD (Santa Cruz Biotechnology, Santa Cruz, CA), and rabbit polyclonal antihuman CEBPA (Abcam). Blots were incubated with secondary horseradish peroxidase-conjugated anti-goat or anti-rabbit antibodies (1:5,000 dilutions; Abcam) and developed using an enhanced chemiluminescence detection kit (Millipore, Billerica, MA). Signal intensity was quantified using an EZ-Capture II chemiluminescence imaging system featuring a charge-cooled camera (Atto Corp., Tokyo, Japan) and measured with the aid of Capture System Analyzer software, version 2.00. Relative protein levels were expressed as the intensity of each protein/intensity of α-tubulin.

Statistical Analyses

The data are expressed as means ± SEMs. Differences between the control and treated groups were evaluated using the general linear model (GLM) of the SAS software (SAS Institute, Cary, NC). A P value < 0.05 was considered to reflect statistical significance. The experiments were done in triplicate, with three replicates in each experiment.

Results

Effect of EGCG on the viability of differentiating BMSCs

The cytotoxic effect of EGCG on differentiating BMSCs was measured using the MTT assay. Cell viability decreased with EGCG concentration in a dose- and time-dependent manner (Figure 1A). Significant inhibition was observed

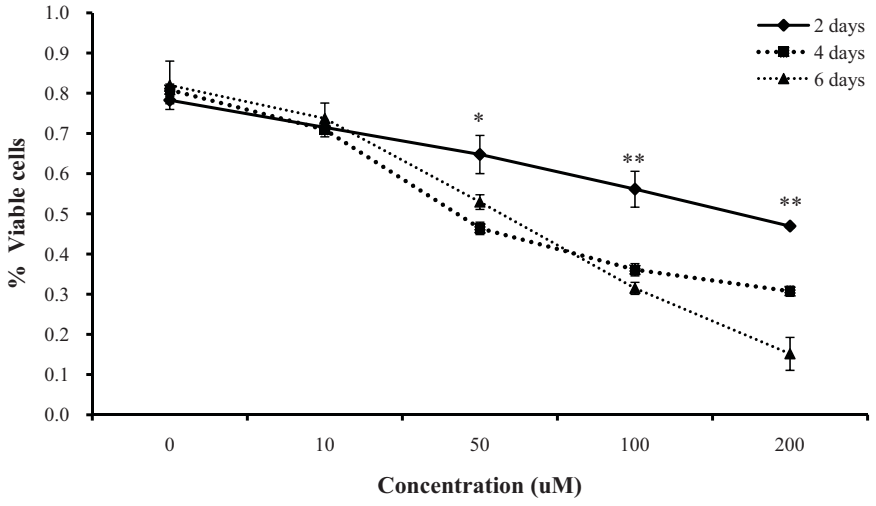

Figure 1 The MTT assay was used to measure cell proliferation at different concentrations of EGCG. The results show that the inhibitory effect of EGCG on BMSC development was dose- and time-dependent. The experiments were performed in triplicate. Values are means ± SEMs. Significant difference: $**P < 0.01$, $*P < 0.05$. The *x*-axis shows the EGCG concentrations and the *y*-axis the percentages of viable cells.

at all EGCG concentrations, i.e., at 50 ($P < 0.05$), 100 ($P < 0.01$), and 200 μM ($P < 0.01$). The extents of inhibition were 71.5%, 64.8%, 56.1%, and 46.9%, respectively, compared to the control at 2 days. The respective figures were 70.9%, 46.4%, 36.1%, and 30.7% at 4 days, and 73.7%, 52.9%, 31.5%, and 15.2% at 6 days. Thus, EGCG suppressed proliferation of differentiating BMSCs in a dose- and time-dependent manner. The work was also done in non-adipogenic differentiation conditions using the MTT assay. Cell viability in non-adipogenic differentiation was not significantly different when treated with these concentrations (Figure 1B).

Effect of EGCG on lipid deposition during differentiation of BMSCs

To explore whether EGCG inhibited lipid deposition in differentiating BMSCs, cells were stained with Oil Red O and the extent of staining was quantitated spectrophotometrically (Figure 2). EGCG significantly reduced lipid deposition in differentiating BMSCs in a dose- and time-dependent manner compared to control cells ($P < 0.01$; Figure 2A). A significant reduction occcurred at 2 days, even at 10 μM ($P < 0.01$). The extent of reduction in staining increased significantly as EGCG levels rose, being almost completely absent at 200 μM EGCG. The percentage of cells staining with Oil Red O respectively at 2 days were 99.7 (control), 91.3, 90.0, 82.9, and 68.8 (rising EGCG levels); 99.7, 90. 8, 78.9, 68. 6, and 48.9 at 4 days; and 99.7, 79.8, 65.9, 44.7, and 22.6 at 6 days (Figure 2B). These data, and our quantitative analysis, show that lipid deposition was diminished in a dose- and time-dependent manner by EGCG, which suppressed lipid droplet accumulation in BMSCs during adipogenic differentiation.

Effect of EGCG on mRNA levels of adipogenic genes during differentiation of BMSCs

We used real-time PCR to explore whether EGCG altered the expression levels of adipogenic genes in differentiating BMSCs. EGCG decreased the mRNA expression levels of the adipogenic genes PPARG, CEBPA, FABP4, and SCD in a dose- and time-dependent manner. The mRNA level of the CEBPA gene did not significantly differ in cultures treated at 10–200 μM EGCG for 2 days (Figure 3A). However, significant differences were observed at 4 and 6 days ($P < 0.01$) compared to control cells. The expression levels of all of PPARG, FABP4, and SCD were significantly reduced by EGCG ($P < 0.05$) (Figure 3B–D). Specifically, the mRNA expression levels of the PPARG, CEBPA, FABP4, and SCD genes at 6 days decreased upon exposure to 10, 50, 100, and 200 μM EGCG compared to 0 μM (Figure 3). Overall, EGCG suppressed the mRNA levels of adipogenic genes.

Effect of EGCG on adipogenic protein expression in differentiating BMSCs

The effects of EGCG on the expression of adipogenic proteins were assessed by Western blotting. Protein extracts of differentiating cells were subjected to immunoblotting. EGCG significantly decreased the levels of the adipogenic enzymes encoded by PPARG, CEBPA, FABP4, and SCD, in a dose-dependent manner, at all time-points tested (Figure 4A). The reductions in protein levels thus mirrored falls in mRNA during adipogenesis (Figure 4B). Consistent with the immunoblotting data, immunolocalization also revealed that EGCG potentially inhibits the expression of both transcription factors (i.e., PPARG and SCD) proteins in differentiating BMSCs (Figure S2). Thus, the mRNA and immunoblotting data show that EGCG inhibited the expression of both transcription factors and adipogenic-specific proteins in a dose- and time-dependent manner.

Effect of EGCG on apoptosis during differentiation of BMSCs

EGCG reduced cell viability, inhibited lipid deposition, and decreased the expression levels of adipogenic genes and proteins. We therefore examined whether the reduction in cell number evident upon EGCG exposure was attributable to apoptosis. Cell death was measured using the TUNEL assay in populations of differentiating BMSCs exposed to various levels of EGCG. TUNEL staining increased in a dose- and time-dependent manner as EGCG levels rose (Figure 5). Cell death may occur by two different mechanisms, i.e., apoptosis and necrosis, but the TUNEL method does not distinguish between them. Thus, to determine whether apoptosis or necrosis was in play, fluorescence-activated cell sorting (FACS) was used to measure differentiating BMSCs with the aid of Annexin V/propidium iodide (PI) staining (Figure 6). EGCG induced both early and late apoptosis, but not necrosis (Figure 6A). Apoptosis (2.2% of cells) was detected at the minimum EGCG dose (10 μM) 2 days after commencement of EGCG exposure (Figure 6B). The percentage of apoptotic cells increased gradually to a maximum of 77.7% (200 μM EGCG) at 6 days ($P < 0.05$). Thus, EGCG-induced apoptosis was positively correlated with viability. Our data clearly indicate that EGCG reduced viability via apoptosis and not necrosis. Thereby, EGCG inhibited the adipogenic differentiation of BMSCs.

Discussion

EGCG suppressed lipid deposition during the differentiation of BMSCs into adipocytes, and our results suggest that an anti-adipogenic capacity of EGCG inhibits adipocyte

Cell Biol Int **39** (2015) 52–64 © 2014 The Authors. Published by John Wiley & Sons Ltd on behalf of the International Federation for Cell Biology.

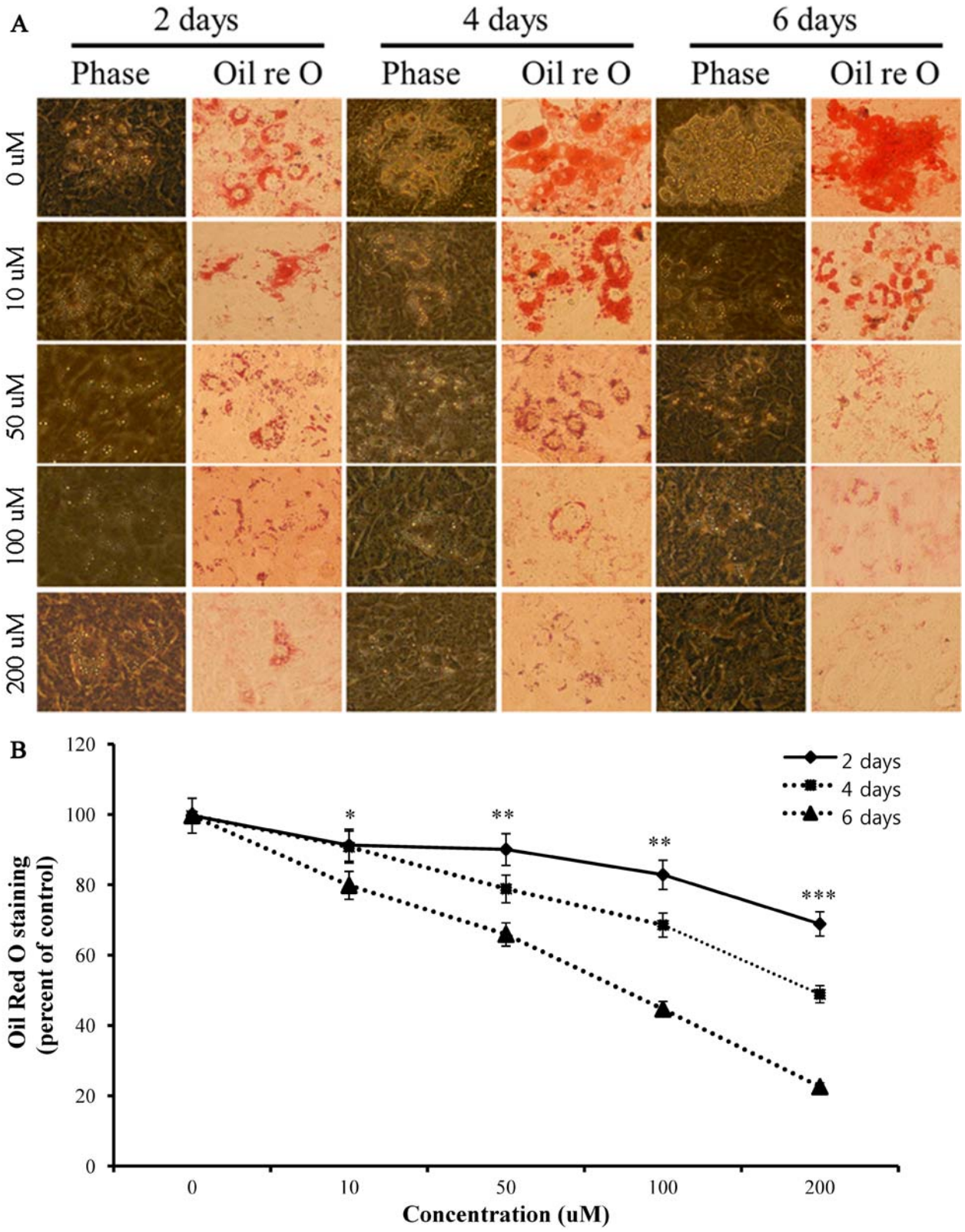

Figure 2 Oil Red O staining to detect adipocytes. Lipid droplet numbers decreased in cells treated with EGCG. (A) Lipid droplets stained with Oil Red O. EGCG treatment significantly reduced lipid deposition in a dose- and time-dependent manner. Test and control cells were examined by phase-contrast microscopy after Oil Red O staining. (B) Numbers of stained cells per microscopic field ($n = 3$). Values are means ± SEMs. The letters in superscript indicate that between-group differences were significant ($P < 0.05$). The *x*-axis shows the EGCG concentrations and the *y*-axis shows the percentages of Oil Red O-stained cells.

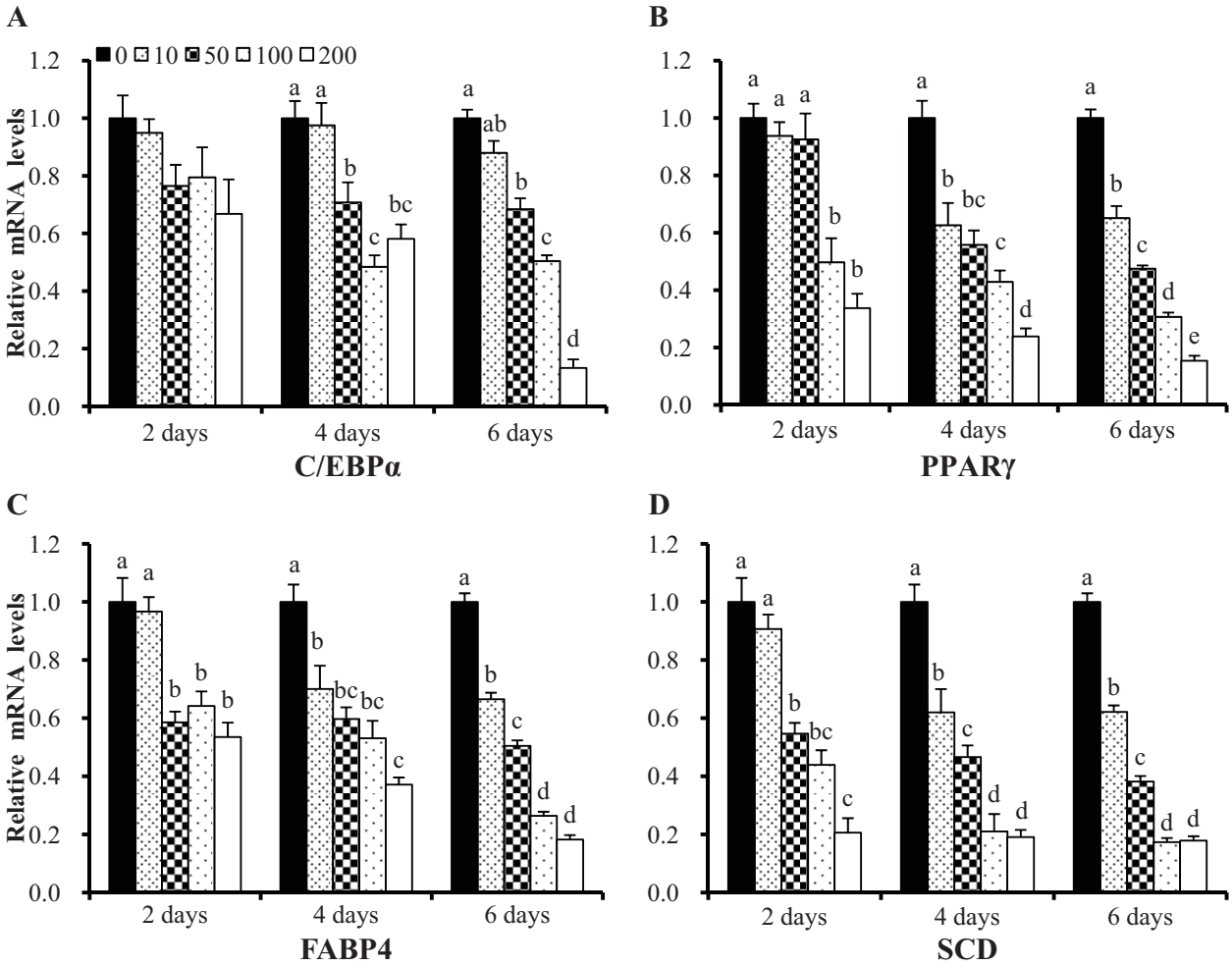

Figure 3 Expression of mRNAs of the PPARG, CEBPA, FABP4, and SCD genes in control BMSCs and cells exposed to various concentrations of EGCG, which lowered the expression levels of all tested genes. mRNA levels were determined by real-time PCR and normalized to those of a housekeeping gene. mRNA levels in control cells were normalized to unity. Values are means ± SEs. Significant difference: $^{**}P < 0.01$.

differentiation. Indeed, EGCG was previously shown to exert an anti-adipogenic effect during cellular differentiation (Liu et al., 2006; Huang et al., 2009; Tang et al., 2012). As EGCG may suppress adipogenesis, we suspected that EGCG might inhibit adipocyte differentiation by regulating BMSC proliferation.

We confirmed that EGCG decreased the level of lipid deposition in differentiating BMSCs, and suggest that inhibition of adipocyte differentiation by EGCG is at least in part attributable to the action of a downregulatory adipogenic factor. EGCG reduced the expression levels of mRNAs associated with adipogenic genes including PPARG, CEBPA, FABP4, and SCD. The transcriptional activities of FABP4 and SCD (genes that regulate the expression levels of enzymes involved in fatty acid synthesis) were reduced upon growth in EGCG. Both FABP4 and SCD are activated by PPARG and CEBPA, which in turn control the expression levels of enzymes used in the synthesis of cholesterol and fatty acids (Proctor et al., 2006; Shin et al., 2007). We thus found that EGCG decreased the expression levels of relevant proteins during adipogenesis.

Our data suggest that the anti-adipogenic effect of EGCG is associated with a reduction in transcriptional activity associated with adipogenesis. In addition, we propose that transcription of FABP4 and SCD is controlled by the same signaling pathway because EGCG reduced transcription from both PPARG and CEBPA. Our findings indicate that EGCG suppresses BMSC pre-adipocyte differentiation by reducing the transcriptional activities of PPARG and CEBPA; both are genes of lipid metabolism. Transcription factors regulate stem cell biology, and the expression of stem cell-associated transcription factors in MSCs has already

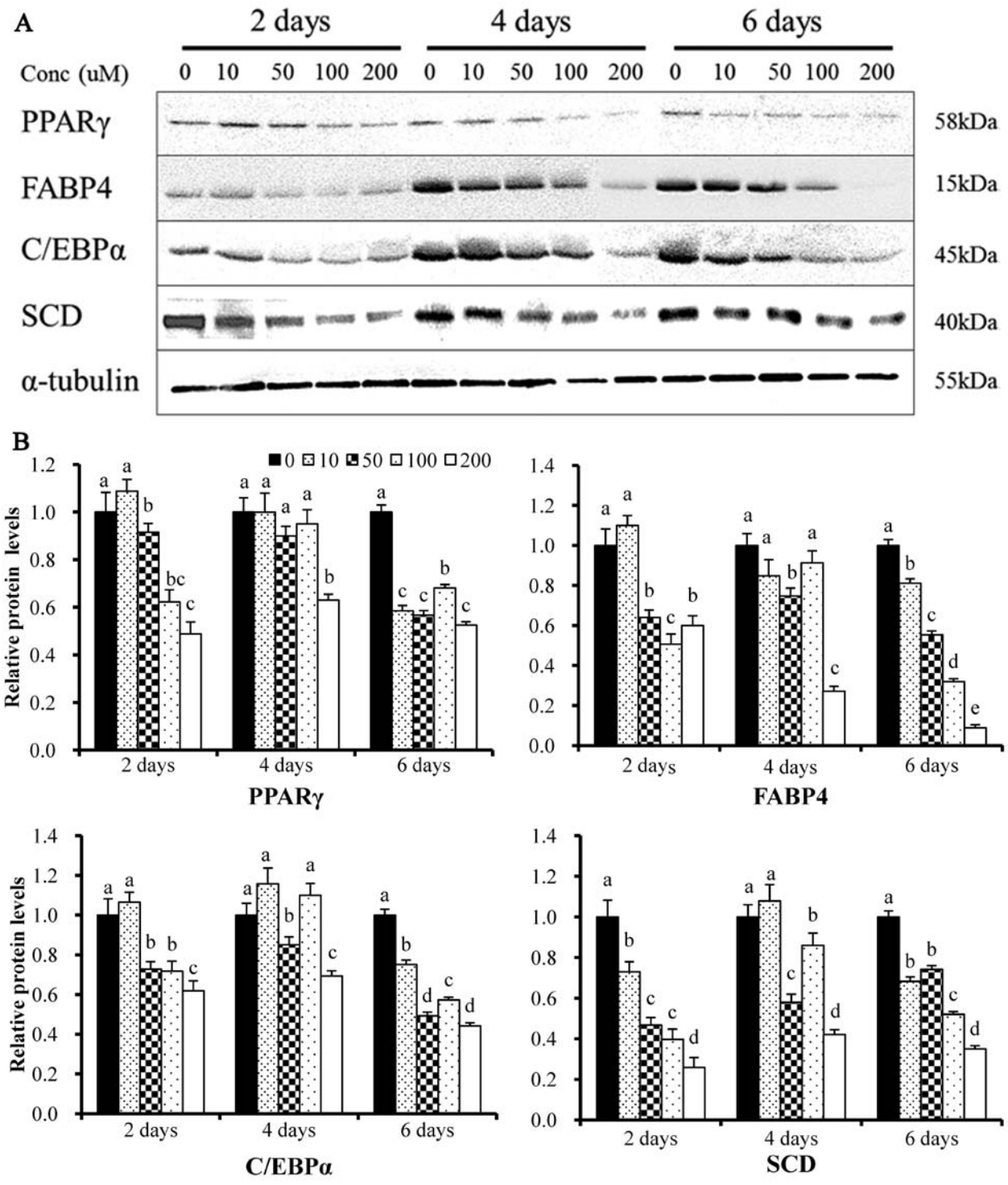

Figure 4 Expression of proteins encoded by the PPARG, CEBPA, FABP4, and SCD genes, and the mRNA levels of these genes in control BMSCs and cells exposed to various concentrations of EGCG, which diminished the expression of all tested genes. mRNA levels were determined by real-time PCR and normalized to those of a housekeeping gene. mRNA levels in control cells were normalized to unity. Values are means ± SEs. Significant difference: $^{**}P < 0.01$.

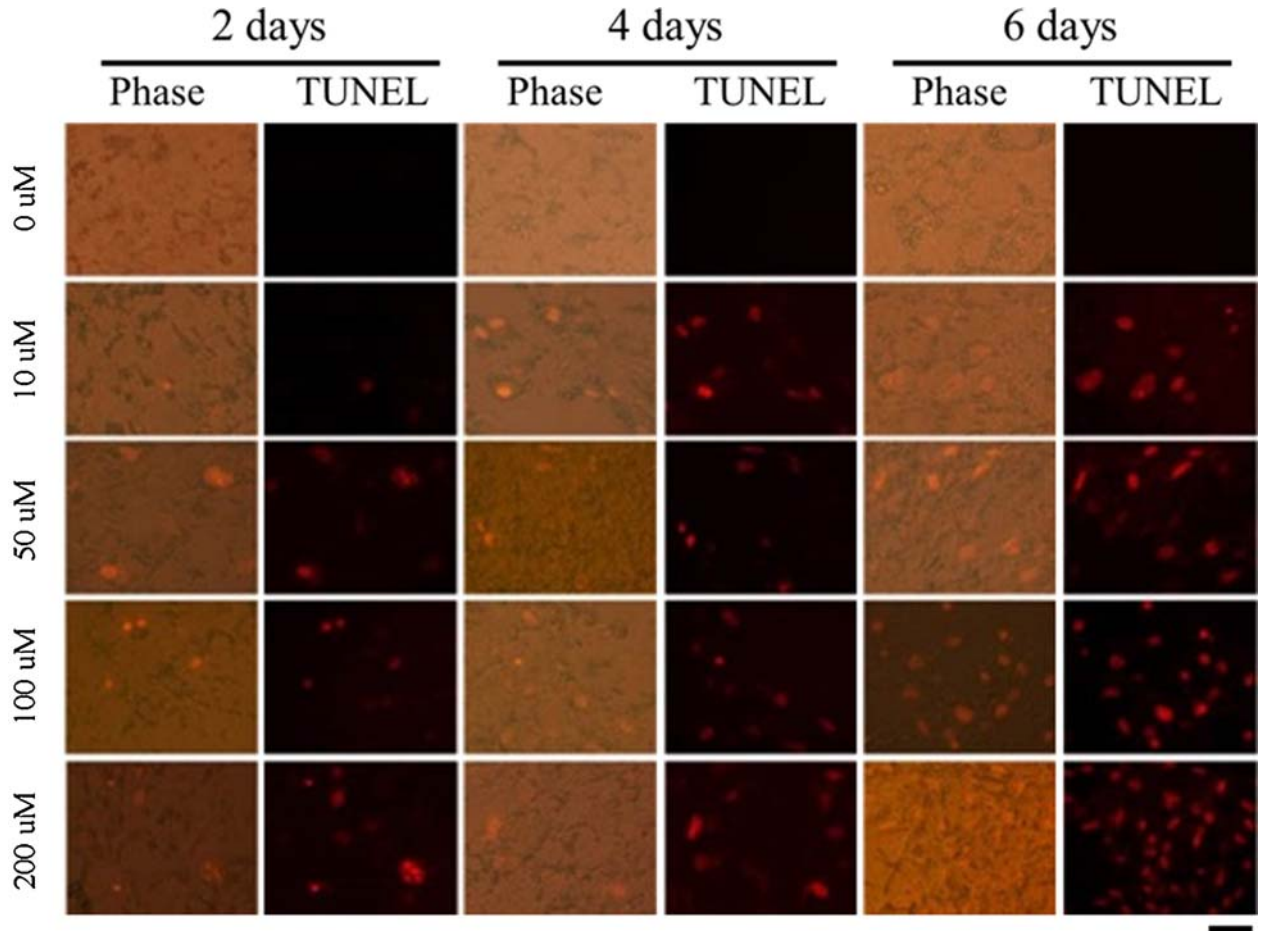

Figure 5 TUNEL assays were performed to measure the extent of apoptosis in BMSCs exposed to EGCG (or not). A representative image of an apoptotic cell is shown (× 100). Apoptosis of BMSCs measured using the TUNEL assay. First row: untreated control cells, second row: cells exposed to 10 μM EGCG, third row: cells exposed to 50 μM EGCG, fourth row: cells exposed to 100 μM EGCG, and fifth row: cells exposed to 200 μM EGCG. In apoptotic cells, cell death appears as a red color. After exposure to EGCG, cells were stained with fluorescein-labeled dUTP according to the protocol described in the Methods. Green fluorescence indicates TUNEL positivity.

been described (Kubo et al., 2009; Ye et al., 2013). EGCG treatment dramatically reduces the mRNA and protein levels of BMSCs. Why do stem cells require such a system? MSCs are multipotent cells of the bone marrow, tendon, and cartilage of fetal and postnatal organisms. This is the first study to explore the effect of EGCG on BMSCs isolated from the bone marrow of fetal cattle.

Human and nonhuman primate cells isolated from bone marrow and adipose tissue are highly homogeneous in terms of cell surface markers. This is consistent with several reports indicating that adult MSCs from various tissues are phenotypically similar (Pittenger et al., 1999; Marquass et al., 2011). Cell surface marker levels did not change markedly after extended passaging of each cell type. Human and other mammalian BMSCs can differentiate into adipogenic, osteogenic, and chondrogenic lineages if the growth media are appropriately supplemented (Hauner et al., 1987; Pittenger et al., 1999; Zuk et al., 2001, 2002). As suggested in previous studies, adult MSCs can also differentiate into multiple lineages including bone, fat, and ectodermal cells (Kang et al., 2004; Izadpanah et al., 2005; Singh et al., 2013). Overall, analyses of BMSCs have shown that they express many factors associated with adipogenesis.

We also explored the effect of EGCG on differentiation of BMSCs during adipogenesis. EGCG has an anti-adipogenic property; the material promotes lipolytic activity via conversion of triglycerides to fatty acids and glycerol (Mochizuki and Hasegawa, 2004; Söhle et al., 2009). We earlier explored how EGCG-induced oxidative stress affected adipogenic differentiation (data not shown), and these observations are in agreement with those of earlier studies (Wei et al., 2011; Yagi et al., 2013). Moreover, the

Cell Biol Int **39** (2015) 52–64 © 2014 The Authors. Published by John Wiley & Sons Ltd on behalf of the International Federation for Cell Biology.

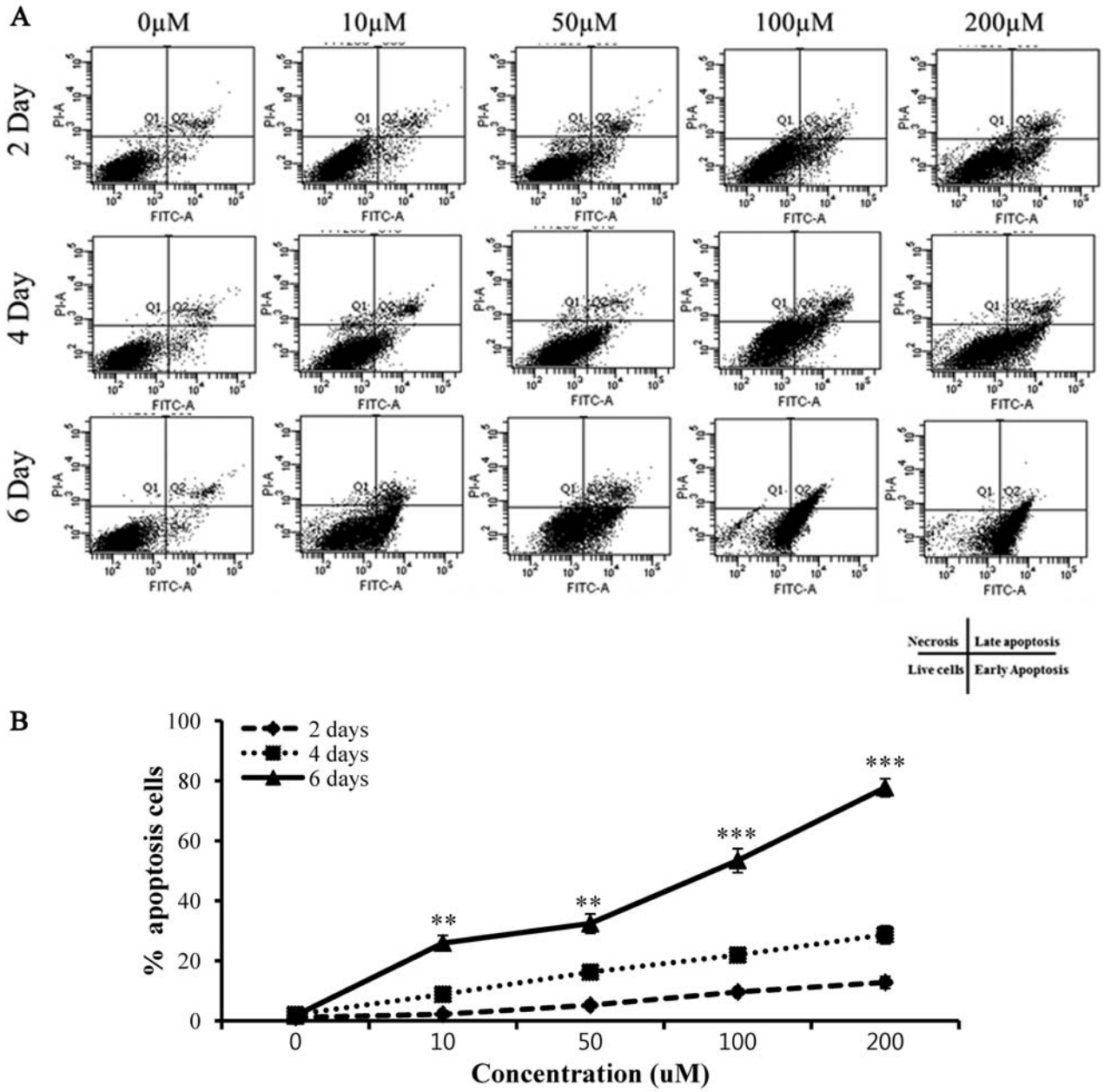

Figure 6 Flow cytometric analysis of differentiating BMSCs treated (or not) with EGCG. (A) The histogram shows dose- and time-dependent reductions in cell viability with concomitant increases in the numbers of Annexin A-positive cells. Phases of the cell cycle were identified via staining with propidium iodide (PI). Apoptosis was quantitated by Annexin V staining. (A) Absorbance of FITC-A: absorbance of fluorescein isothiocyanate–Annexin V (Please clarify). Q1: necrosis, Q2: late apoptosis, Q3: live cells, Q4: early apoptosis. (B) The percentages of apoptosis in cultures exposed (or not) to various concentrations of EGCG. This material triggered cell-cycle arrest and apoptosis in a time- and dose-dependent manner. Values are means ± SEMs. The letters in superscript indicate that the difference between groups was significant ($P < 0.05$). The *x*-axis shows the EGCG concentrations and the *y*-axis shows the percentages of apoptotic cells. The upper-right quadrant contains data on cells positive for both Annexin V and PI, and the lower-right quadrant shows quadrant information on cells positive for Annexin V but negative for PI.

transcription factors PPARG and CEBPA are important in the early stage of adipocyte differentiation. CEBPA induces adipogenesis via PPARG (Rosen, 2005). The 2 transcription factors mentioned regulate numerous genes required for adipogenic differentiation of BMSCs (Hauner et al., 1987; Zou et al., 2008). In agreement with previous studies, we found that EGCG induced dose- and time-dependent suppression of mRNAs and proteins of the PPARG, CEBPA,

FABP4, and SCD genes in differentiating adipocytes. EGCG suppressed expression of both the encoding mRNAs, and the proteins per se, of adipogenic transcription factors, in turn inhibiting adipocyte differentiation (Moon et al., 2007). PPARG is a key transcription factor in terms of induction of adipogenesis and lipid accumulation (Kim et al., 2003). EGCG-mediated downregulation of PPARG expression would be expected to be inhibitory to lipid deposition and adipocyte differentiation.

EGCG-mediated inhibition of adipogenesis was noted at all time-points (2, 4, and 6 days). This clearly shows that EGCG inhibits the proliferation of pre-adipocytes and prevents differentiation of such cells into mature adipocytes. EGCG also significantly affected the mRNA and protein levels of the FABP4 and SCD genes, further indicating that EGCG inhibits both early and late adipogenesis. Both FABP4 and SCD are very important in the context of lipogenesis and adipogenic differentiation, regulating fatty acid synthesis and release, and insulin signaling. Here, we showed immunocytochemically a markedly lower lipid localization in differentiating BMSCs compared with the control. EGCG-mediated suppression of mRNA and protein levels may be attributable to a direct effect of EGCG on apoptosis; EGCG increased apoptosis in skin tumors of mice (Lu et al., 2002), and it suppressed cell viability and induced apoptosis of human breast carcinoma MCF-7 cells (Mittal et al., 2004). EGCG regulates the expression of apoptotic genes and mediates anti-adipogenic activity via the WNT/β-catenin pathway (Lee et al., 2013). These observations indicate that EGCG directly or indirectly affects apoptosis and suppresses adipogenesis.

Annexin V and TUNEL staining showed that EGCG actively induced apoptosis at both the early and late stages of adipogenesis. This may be attributable to a dose- and time-dependent stimulation of reactive oxygen species (ROS) and reactive nitrogen species (RNS) synthesis by EGCG, in turn stimulating formation of highly reactive peroxynitrites that initiate lipid peroxidation, externalization of phosphatidylserine, DNA damage, and activation of caspase-3. The latter step would trigger apoptosis of differentiating adipocytes. Consistent with Wang et al. (2009); our data support the notion that exposure to EGCG increases apoptosis by stimulating production of ROS and nitrous oxide (NO; Hsuuw and Chan, 2007; Park et al., 2013). EGCG inhibits adipogenesis by suppressing lipid deposition and by inhibiting the expression of adipogenic genes and proteins. We suggest that EGCG inhibits apoptosis via both ROS production and an NO-dependent mechanism. However, more work is required to better understand the effects of EGCG on apoptotic signaling during adipogenic differentiation of BMSCs. This may improve the treatment of obesity. Nevertheless, our present study already suggests that EGCG may be useful in this context.

In conclusion, EGCG exhibited anti-adipogenic effects on BMSCs. EGCG caused apoptosis to increase markedly during differentiation and inhibited the expression of adipogenic genes and proteins, in turn significantly suppressing adipogenic differentiation. An increase in apoptosis was a key feature of the anti-adipogenic effect of EGCG.

Acknowledgements

This study was supported by Postdoctoral Fellowship Program (Project No: PJ008487) of the National Livestock Research Institute and BioGreen 21 Program (Project No: PJ00819101) of Rural Development Administration, Republic of Korea.

References

Aust L, Devlin B, Foster SJ, Halvorsen YD, Hicok K, du Laney T, Sen A, Willingmyre GD, Gimble JM (2004) Yield of human adipose-derived adult stem cells from liposuction aspirates. Cytotherapy 6: 7–14.

Basu A, Sanchez K, Leyva MJ, Wu M, Betts NM, Aston CE, Lyons TJ (2010) Green tea supplementation affects body weight, lipids, and lipid peroxidation in obese subjects with metabolic syndrome. J Am Coll Nutr 29: 31–40.

Boeloni JN, Ocarino NM, Melo AB, Silva JF, Castanheira P, Goes AM, Serakides R (2009) Dose-dependent effects of triiodothyronine on the osteogenic differentiation of rat bone marrow mesenchymal stem cells. Horm Res 72: 88–97.

Boschmann M, Thielecke F (2007) The effects of epigallocatechin-3-gallate on thermogenesis and fat oxidation in obese men: a pilot study. J Am Coll Nutr 26: 389S–95S.

Byun JK, Yoon BY, Jhun JY, Oh HJ, Kim EK, Min JK, Cho ML (2014) Epigallocatechin-3-gallate ameliorates both obesity and autoinflammatory arthritis aggravated by obesity by altering the balance among CD4(+) T-cell subsets. Immunol Lett 157: 51–9.

Chan CY, Wei L, Castro-Muñozledo F, Koo WL (2011) (−)-Epigallocatechin-3-gallate blocks 3T3-L1 adipose conversion by inhibition of cell proliferation and suppression of adipose phenotype expression. Life Sci 89: 779–85.

Collett GD, Canfield AE (2005) Angiogenesis and pericytes in the initiation of ectopic calcification. Circ Res 96: 930–8.

Doherty MJ, Ashton BA, Walsh S, Beresford JN, Grant ME, Canfield AE (1998) Vascular pericytes express osteogenic potential in vitro and in vivo. J Bone Miner Res 13: 828–38.

Farrington-Rock C, Crofts NJ, Doherty MJ, Ashton BA, Griffin-Jones C, Canfield AE (2004) Chondrogenic and adipogenic potential of microvascular pericytes. Circulation 110: 2226–32.

Friedenstein AJ, Chailakhyan RK, Latsinik NV, Panasyuk AF, Keiliss-Borok IV (1974) Stromal cells responsible for transferring the microenvironment of the hemopoietic tissues. Cloning in vitro and retransplantation in vivo. Transplantation 17: 331–40.

Friedenstein AJ, Gorskaja JF, Kulagina NN (1976) Fibroblast precursors in normal and irradiated mouse hematopoietic organs. Exp Hematol 4: 267–74.

Geng J, Peng F, Xiong F, Shang Y, Zhao C, Li W, Zhang C (2009) Inhibition of myostatin promotes myogenic differentiation of rat bone marrow-derived mesenchymal stromal cells. Cytotherapy 11: 849–63.

Glynn MW, McAllister AK (2006) Immunocytochemistry and quantification of protein colocalization in cultured neurons. Nat Protoc 1: 1287–96.

Hauner H, Schmid P, Pfeiffer EF (1987) Glucocorticoids and insulin promote the differentiation of human adipocyte precursor cells into fat cells. J Clin Endocrinol Metab 64: 832–5.

Hsuuw YD, Chan WH (2007) Epigallocatechin gallate dose-dependently induces apoptosis or necrosis in human MCF-7 cells. Ann N Y Acad Sci 1095: 428–40.

Huang CH, Tsai SJ, Wang YJ, Pan MH, Kao JY, Way TD (2009) EGCG inhibits protein synthesis, lipogenesis, and cell cycle progression through activation of AMPK in p53 positive and negative human hepatoma cells. Mol Nutr Food Res 53: 1156–65.

Izadpanah R, Joswig T, Tsien F, Dufour J, Kirijan JC, Bunnell BA (2005) Characterization of multipotent mesenchymal stem cells from the bone marrow of rhesus macaques. Stem Cells Dev 14: 440–51.

Kang SK, Putnam L, Dufour J, Ylostalo J, Jung JS, Bunnell BA (2004) Expression of telomerase extends the lifespan and enhances osteogenic differentiation of adipose tissue-derived stromal cells. Stem Cells 22: 1356–72.

Kim MS, Kim JK, Kim HJ, Moon SR, Shin BC, Park KW, Yang HO, Kim SM, Park R (2003) Hibiscus extract inhibits the lipid droplet accumulation and adipogenic transcription factors expression of 3T3-L1 preadipocytes. J Altern Complement Med 9: 499–504.

Ku HC, Chang HH, Liu HC, Hsiao CH, Lee MJ, Hu YJ, Hung PF, Liu CW, Kao YH (2009) Green tea (−)-epigallocatechin gallate inhibits insulin stimulation of 3T3-L1 preadipocyte mitogenesis via the 67-kDa laminin receptor pathway. Am J Physiol Cell Physiol 297: C121–32.

Kubo H, Shimizu M, Taya Y, Kawamoto T, Michida M, Kaneko E, Igarashi A, Nishimura M, Segoshi K, Shimazu Y, Tsuji K, Aoba T, Kato Y (2009) dentification of mesenchymal stem cell (MSC)-transcription factors by microarray and knockdown analyses, and signature molecule-marked MSC in bone marrow by immunohistochemistry. Genes Cells 14: 407–24.

Lee H, Bae S, Yoon Y (2013) The anti-adipogenic effects of (−) epigallocatechin gallate are dependent on the WNT/β-catenin pathway. J Nutr Biochem 24: 1232–40.

Liu HS, Chen YH, Hung PF, Kao YH (2006) Inhibitory effect of green tea (−)-epigallocatechin gallate on resistin gene expression in 3T3-L1 adipocytes depends on the ERK pathway. Am J Physiol Endocrinol Metab 290: E273–81.

Livak KJ, Schmittgen TD (2001) Analysis of relative gene expression data using real-time quantitative PCR and the 2 (-Delta Delta C(T)) Method. Methods 25: 402–8.

Lu YP, Lou YR, Xie JG, Peng QY, Liao J, Yang CS, Huang MT, Conney AH (2002) Topical applications of caffeine or (−)-epigallocatechin gallate (EGCG) inhibit carcinogenesis and selectively increase apoptosis in UVB-induced skin tumors in mice. Proc Natl Acad Sci U S A 99: 12455–60.

Marquass B, Schulz R, Hepp P, Zscharnack M, Aigner T, Schmidt S, Stein F, Richter R, Osterhoff G, Aust G, Josten C, Bader A (2011) Matrix-associated implantation of predifferentiated mesenchymal stem cells versus articular chondrocytes: in vivo results of cartilage repair after 1 year. Am J Sports Med 39: 1401–12.

Menssen A, Häupl T, Sittinger M, Delorme B, Charbord P, Ringe J (2011) Differential gene expression profiling of human bone marrow-derived mesenchymal stem cells during adipogenic development. BMC Genomics 12: 461.

Mielgo-Ayuso J, Barrenechea L, Alcorta P, Larrarte E, Margareto J, Labayen I (2013) Effects of dietary supplementation with epigallocatechin-3-gallate on weight loss, energy homeostasis, cardiometabolic risk factors and liver function in obese women: randomised, double-blind, placebo-controlled clinical trial. Br J Nutr 3 2013; 1–9.

Mittal A, Pate MS, Wylie RC, Tollefsbol TO, Katiyar SK (2004) EGCG down-regulates telomerase in human breast carcinoma MCF-7 cells, leading to suppression of cell viability and induction of apoptosis. Int J Oncol 24: 703–10.

Mochizuki M, Hasegawa N (2004) Effects of green tea catechin-induced lipolysis on cytosol glycerol content in differentiated 3T3-L1 cells. Phytother Res 18: 945–6.

Moon HS, Chung CS, Lee HG, Kim TG, Choi YJ, Cho CS (2007) Inhibitory effect of (−)-epigallocatechin-3-gallate on lipid accumulation of 3T3-L1 cells. Obesity (Silver Spring) 15: 2571–82.

Moseley VR, Morris J, Knackstedt RW, Wargovich MJ (2013) Green Tea Polyphenol Epigallocatechin 3-Gallate, Contributes to the Degradation of DNMT3A and HDAC3 in HCT 116 Human Colon Cancer Cells. Anticancer Res 33: 5325–33.

Park SY, Jeong YJ, Kim SH, Jung JY, Kim WJ (2013) Epigallocatechin gallate protects against nitric oxide-induced apoptosis via scavenging ROS and modulating the Bcl-2 family in human dental pulp cells. J Toxicol Sci 38: 371–8.

Pittenger MF, Mackay AM, Beck SC, Jaiswal RK, Douglas R, Mosca JD, Moorman MA, Simonetti DW, Craig S, Marshak DR (1999) Multilineage potential of adult human mesenchymal stem cells. Science 284: 143–7.

Proctor G, Jiang T, Iwahashi M, Wang Z, Li J, Levi M (2006) egulation of renal fatty acid and cholesterol metabolism, inflammation, and fibrosis in Akita and OVE26 mice with type 1 diabetes. Diabetes 55: 2502–9.

Renno WM, Al-Maghrebi M, Alshammari A, George P (2013) (−)-Epigallocatechin-3-gallate (EGCG) attenuates peripheral nerve degeneration in rat sciatic nerve crush injury. Neurochem Int 62: 221–31.

Rosen ED (2005) The transcriptional basis of adipocyte development. Prostaglandins Leukot Essent Fatty Acids 73: 31–4.

Schreml S, Babilas P, Fruth S, Orsó E, Schmitz G, Mueller MB, Nerlich M, Prantl L (2009) Harvesting human adipose tissue-derived adult stem cells: resection versus liposuction. Cytotherapy 11: 947–57.

Shin ES, Lee HH, Cho SY, Park HW, Lee SJ, Lee TR (2007) Genistein downregulates SREBP-1 regulated gene expression by inhibiting site-1 protease expression in HepG2 cells. J Nutr 137: 1127–31.

Shin J, Li B, Davis ME, Suh Y, Lee K (2009) Comparative analysis of fatty acid-binding protein 4 promoters: conservation of peroxisome proliferator-activated receptor binding sites. J Anim Sci 87: 3923–34.

Simmons DJ, Seitz P, Kidder L, Klein GL, Waeltz M, Gundberg CM, Tabuchi C, Yang C, Zhang RW (1991) Partial characterization of rat marrow stromal cells. Calcif Tissue Int 48: 326–34.

Singh SP, Tripathy NK, Nityanand S (2013) Comparison of phenotypic markers and neural differentiation potential of multipotent adult progenitor cells and mesenchymal stem cells. World J Stem Cells 5: 53–60.

Söhle J, Knott A, Holtzmann U, Siegner R, Grönniger E, Schepky A, Gallinat S, Wenck H, Stäb F, Winnefeld M (2009) White Tea extract induces lipolytic activity and inhibits adipogenesis in human subcutaneous (pre)-adipocytes. Nutr Metab (Lond) 6: 20.

Tang QQ, Lane MD (2012) Adipogenesis: from stem cell to adipocyte. Annu Rev Biochem 81: 715–36.

Toolsee NA, Aruoma OI, Gunness TK, Kowlessur S, Dambala V, Murad F, Googoolye K, Daus D, Indelicato J, Rondeau P, Bourdon E, Bahorun T (2013) Effectiveness of green tea in a randomized human cohort: relevance to diabetes and its complications. Biomed Res Int 2013: 412379.

Valenti D, De Rasmo D, Signorile A, Rossi L, de Bari L, Scala I, Granese B, Papa S, Vacca RA (2013) Epigallocatechin-3-gallate prevents oxidative phosphorylation deficit and promotes mitochondrial biogenesis in human cells from subjects with Down's syndrome. Biochim Biophys Acta 1832: 542–52.

Wang X, Hao MW, Dong K, Lin F, Ren JH, Zhang HZ (2009) Apoptosis induction effects of EGCG in laryngeal squamous cell carcinoma cells through telomerase repression. Arch Pharm Res 32: 1263–9.

Wei IH, Tu HC, Huang CC, Tsai MH, Tseng CY, Shieh JY (2011) (−)-Epigallocatechin gallate attenuates NADPH-d/nNOS expression in motor neurons of rats following peripheral nerve injury. BMC Neurosci 12: 52.

Yagi H, Tan J, Tuan RS (2013) Polyphenols suppress hydrogen peroxide-induced oxidative stress in human bone-marrow derived mesenchymal stem cells. J Cell Biochem 114: 1163–73.

Yang J, Li L, Tan S, Jin H, Qiu J, Mao Q, Li R, Xia C, Jiang ZH, Jiang S, Liu S (2012) A natural theaflavins preparation inhibits HIV-1 infection by targeting the entry step: potential applications for preventing HIV-1 infection. Fitoterapia 83: 348–55.

Ye X, Yan T, Chopp M, Zacharek A, Ning R, Venkat P, Roberts C, Chen J. (2013) Combination BMSC and Niaspan Treatment of Stroke Enhances White Matter Remodeling and Synaptic Protein Expression in Diabetic Rats. Int J Mol Sci 14: 22221–32.

Zou L, Zou X, Chen L, Li H, Mygind T, Kassem M, Bünger C (2008) Multilineage differentiation of porcine bone marrow stromal cells associated with specific gene expression pattern. J Orthop Res 26: 56–64.

Zuk PA, Zhu M, Mizuno H, Huang JI, Chaudhari S, Lorenz HP, Benhaim P, Hedrick MH (2001) Multilineage cells derived from human adipose tissue, a putative source of stem cells for tissue engineering. Tissue Eng 7: 211–6.

Zuk PA, Zhu M, Ashjian P, De Ugarte DA, Huang JI, Mizuno H, Alfonso ZC, Fraser JK, Benhaim P, Hedrick MH (2002) Human adipose tissue is a source of multipotent stem cells. Mol Biol Cell 13: 4279–95.

Received 7 January 2014; accepted 9 June 2014.
Final version published online 14 August 2014.

Supporting Information

Additional supporting information may be found in the online version of this article at the publisher's web-site.

Figure S1: The MTT assay was used to measure cell proliferation in non-adipogenic differentiation. The results show that the effect of EGCG on non-adipogenic differentiation was not difference at dose- and time-dependent. The x-axis shows the EGCG concentrations and the y-axis the percentages of viable cells.

Figure S2: The immunolocalization of PPARG and SCD proteins in control and various EGCG exposed groups. The green colour indicates the immunolocalization of SCD, red colour indicates the localization of PPARG, and the blue indicates the nucleus by DAPI staining.